ACS OMEGA

Open Access

http://pubs.acs.org/journal/acsodf

Article

Experimental Results and Mechanistic Insights on the Reactions of Indolylmethyl Acetates with Soft Carbon Pronucleophiles

Antonio Arcadi, Massimiliano Aschi, Marco Chiarini, Giancarlo Fabrizi,* Andrea Fochetti, Antonella Goggiamani, Federica Iavarone, Antonia Iazzetti,* Andrea Serraiocco, and Roberta Zoppoli

Cite This: https://doi.org/10.1021/acsomega.4c02409

Read Online

ACCESS | Metrics & More | Article Recommendations | Supporting Information

ABSTRACT: The palladium-catalyzed reaction of *N*-protected 2-indolylmethyl acetates with soft carbon pronucleophiles is described. Besides the formation of the expected coupling reaction at the C1′ position, unprecedented attack at the C3 position of the plausible η^3-indolyl-palladium intermediate has been observed, and the selectivity control C1′/C3 seems to depend on the nature of the protecting group and ligand. The reactivity of 3-indolylmethyl acetates has also been also investigated. Quantum chemical calculations support the experimental results.

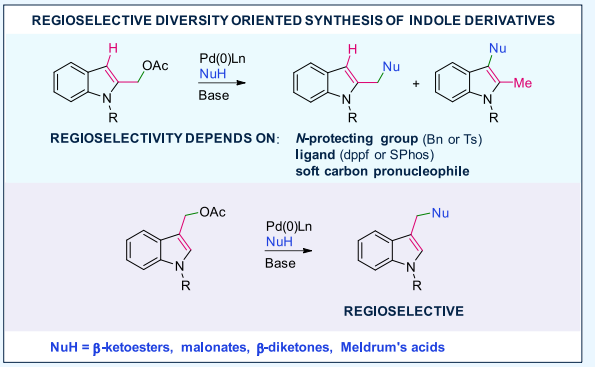

INTRODUCTION

The wide spectrum of applications in medicinal chemistry, dye industry, material science, and agriculture of indoles continues to render the development of diversity-oriented synthesis of these scaffolds a very active research area.[1] In particular, the functionalization of the preformed indole ring with groups prone to undergo easy further elaboration represents a powerful tool to approach a variety of synthetic targets of great relevance in drug discovery.[2] Significantly, the use of indole-2-carbinols and indole-3-carbinols[3] and derivatives[4] as starting building blocks found wide applications for the preparation of chiral indole-based heterocycles.[5] In this context, we described the functionalization of benzofurans through Tsuji−Trost-type reactions involving a palladium-catalyzed benzylic-like nucleophilic substitution exclusively at the exomethyl position (Scheme 1a).[6] The palladium-catalyzed reaction of indolylmethyl or benzofuranylmethyl acetates with boronic acids accomplished an easy approach to indole/benzofuran-containing diarylmethanes (Scheme 1b).[7]

Functionalization of the (1*H*-indol-2-yl)methyl acetates with N, O, and S soft nucleophiles and (1*H*-indol-3-yl)methyl acetates with secondary amines under metal-free conditions could also occur. Very likely, activated carbinols should be respectively precursors of transient indole methides I and II that could be trapped by different nucleophiles. ESI-MS and IR multiple-photon dissociation (IRMPD) spectroscopy analysis provided evidence about a conjugate addition of the nucleophile to 2-alkylideneindolenines I and 3-alkylideneindoleninium II (Scheme 2).[8]

Furthermore, as part of our ongoing interest in the synthesis of nitrogen-containing polycyclic scaffolds, we explored the sequential reactions of **1** with α-amino acids to afford 3-substituted 2,3-dihydropyrazino[1,2-*a*]indol-4(1*H*)-ones **2** (Scheme 3a).[9] Analogously, the domino palladium-catalyzed reaction of indol-2-ylmethyl acetates with 1,3-dicarbonyls achieved the synthesis of 1,2-dihydro-3*H*-pyrrolo[1,2-*a*]indol-3-ones **3** (Scheme 3b).[10]

We envisaged that the reaction of suitable *N*-substituted-(1*H*-indolyl)methyl acetates **4** and **8** with carbon soft pronucleophiles can achieve the diversity-oriented synthesis of the corresponding indole derivatives (Scheme 4).

Although it is well-known that these types of substrates could generate the η^3-indolyl-palladium intermediate or alkylideneindolenines, to the best of our knowledge the functionalization with β-ketoesters, 1,3-dicarbonyl compounds, malonates, and Meldrum's acids has not been examined in detail.[11]

We supposed that computational studies could have accomplished insights into the different reaction pathways, helping to address the product selectivity control and highlighting the key role of the palladium catalysis for the reaction outcome.

Herein we report the results of our investigation.

Received: March 12, 2024
Revised: April 15, 2024
Accepted: April 19, 2024

Scheme 1. (a) Benzofuran Functionalization through Palladium-Catalyzed Tsuji−Trost-Type Reactions; (B) Palladium-Catalyzed Reaction of Indolylmethyl or Benzofuranylmethyl Acetates with Boronic Acids

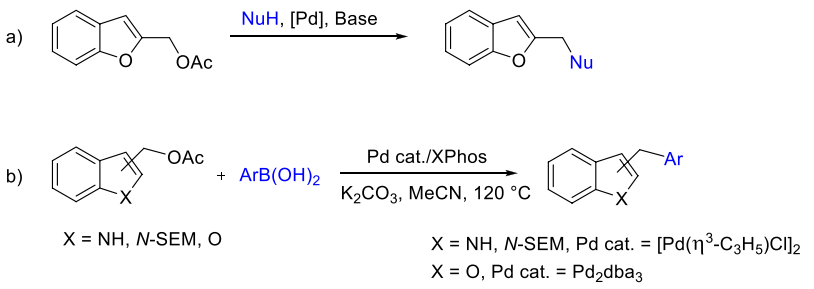

Scheme 2. Conjugate Addition-Type Reactions of Nucleophiles to the in Situ Generated Alkylideneindolenines I and Alkylideneindolinium Ions II

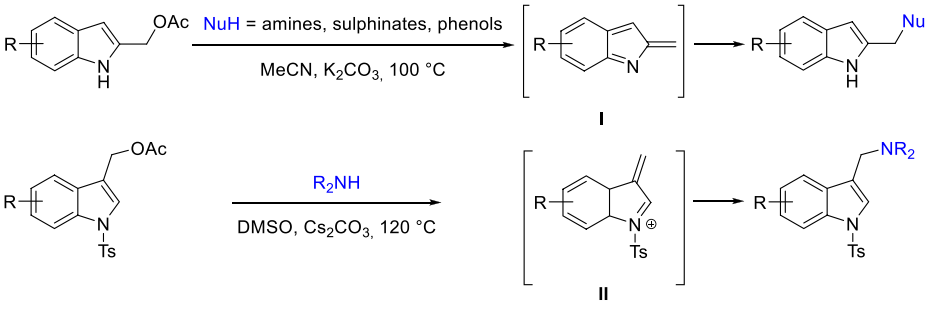

Scheme 3. Base-Promoted (a) and Palladium-Catalyzed (b) Domino Reactions of 2-Indolylmethyl Acetates 1 with α-Amino Acids and 1,3-Dicarbonyls, Respectively

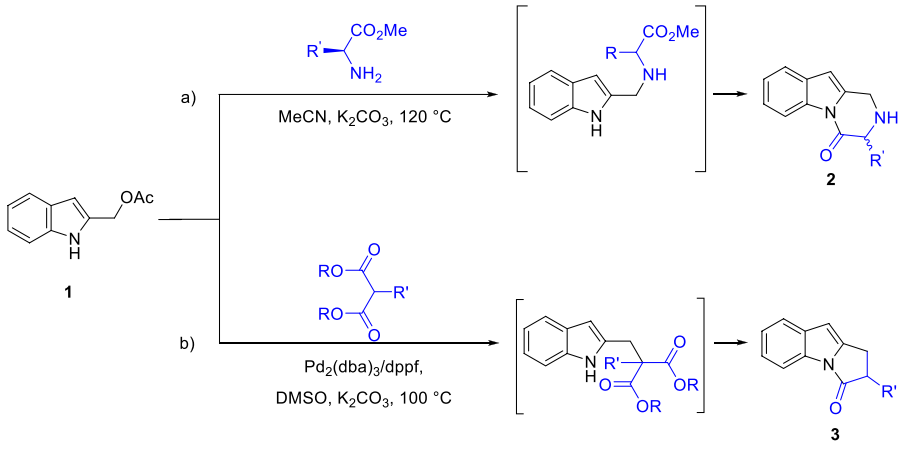

Scheme 4. Present Work

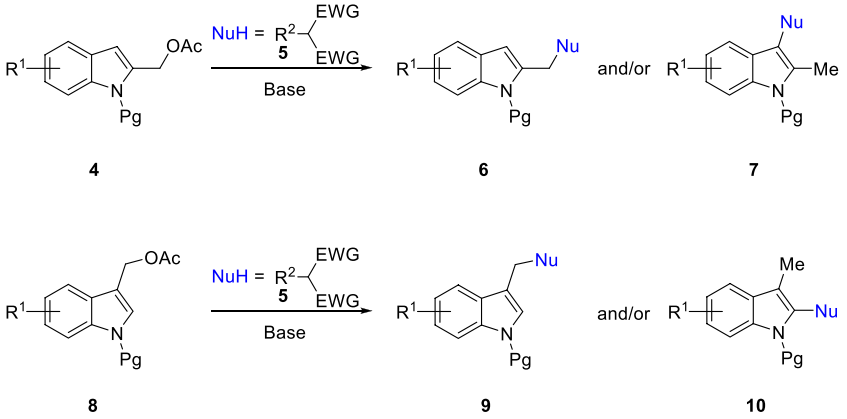

https://doi.org/10.1021/acsomega.4c02409
ACS Omega XXXX, XXX, XXX−XXX

Scheme 5. C1′ vs C3 Nucleophilic Attack

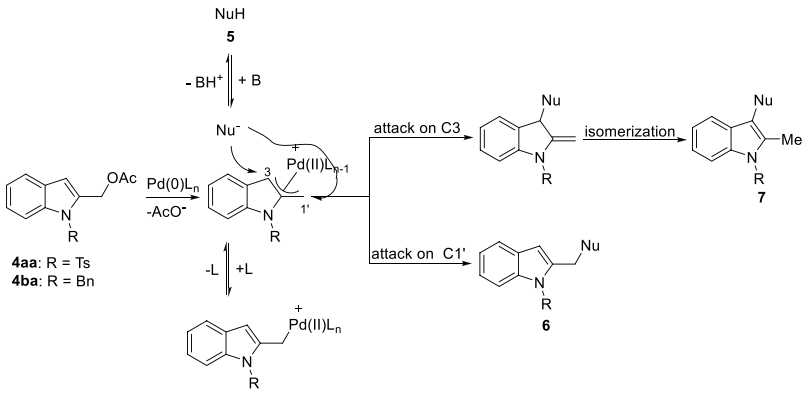

Table 1. Optimization Studies for the Reaction of 4aa with Ethyl 2-Methyl-3-oxobutenoate 5a[a]

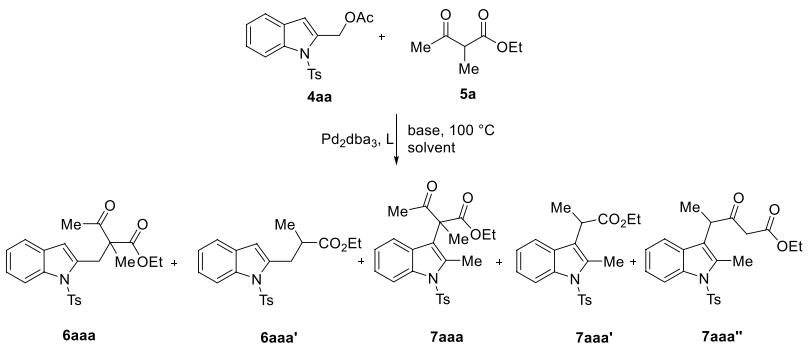

Entry[b]	Ligand	Solvent	Base	t (h)	6aaa (%)	6aaa′ (%)	7aaa (%)	7aaa′ (%)	7aaa″ (%)	Overall yield (%)	C1′/C3
1	dppf	DMSO	Li_2CO_3	24	0	5	0	1		6	83/17
2	dppf	DMSO	Cs_2CO_3	5	27	19	21	8		75	60/40
3	dppf	DMSO	K_2CO_3	24	19	21	19	8		67	60/40
4	dppf	THF	NaH	5.5	13	2	3	1		19	74/26
5	dppf	THF	K_2CO_3/NaH	24	0	37	0	12		49	75/25
6	dppf	DMF	NaH	24	29	3	33	1	traces	66	49/51
7	dppf	DMF	K_2CO_3/NaH	24	32	8	36	5	traces	81	49/51
8	dppf	DMSO	K_2CO_3/NaH	24	31	14	34	6	13	98	46/54
9	dppm	DMSO	K_2CO_3/NaH	24							
10	dppe	DMSO	K_2CO_3/NaH	24	34	6	16	3	6	65	67/33
11	dppp	DMSO	K_2CO_3/NaH	4	54	6	30		10	100	60/40
12	XantPhos	DMSO	K_2CO_3/NaH	3.5	16	5	56	7	16	100	21/79
13	DavePhos	DMSO	K_2CO_3/NaH	3	16	8	53	5	17	99	24/76
14	XPhos	DMSO	K_2CO_3/NaH	64	6		28		8	42	14/86
15[c]	DavePhos	DMSO	K_2CO_3/NaH	2	10	1	41	6	6	67	30/70
16[c,d]	DavePhos	DMSO	K_2CO_3/NaH	26	5	6	15	7		33	33/67
17	RuPhos	DMSO	K_2CO_3/NaH	3	12	5	43	9	12	81	27/73
18	SPhos	DMSO	K_2CO_3/NaH	3	11		55	8	17	92	12/88
19	MePhos	DMSO	K_2CO_3/NaH	24		12		8		20	74/26
20	JohnPhos	DMSO	K_2CO_3/NaH	24	2	9	8	7		26	59/41
21	(*o*-furyl)$_3$P	DMSO	K_2CO_3/NaH	24							
22	TTTP	DMSO	K_2CO_3/NaH	3.5	31	3	39	3	24	100	34/66
23	(*t*-Bu)$_3$PHBF$_4$	DMSO	K_2CO_3/NaH	24	4	11				15	100/0
24	*t*-BuXPhos	DMSO	K_2CO_3/NaH	24		3		3		6	87/13
25	*t*-BuXantPhos	DMSO	K_2CO_3/NaH	24		8		2		10	93/7

[a]Unless otherwise stated, reactions were carried out on a 0.30 mmol scale under an argon atmosphere using 0.02 equiv of Pd_2dba_3, 0.08 equiv of monodentate ligand or 0.04 of bidentate ligand, 1.5 equiv of **5a**, 1.5 equiv of M_2CO_3 and 1.7 equiv of NaH when present in 2.5 mL of anhydrous solvent at 100 °C. [b]Yields are given for isolated products. [c]Reaction was carried out with $[Pd(C_3H_5)Cl]_2$. [d]Reaction was carried out with preformed sodium salt of **5a**.

https://doi.org/10.1021/acsomega.4c02409
ACS Omega XXXX, XXX, XXX−XXX

Table 2. Reaction of 4ba with Ethyl 2-Methyl-3-oxobutenoate 5a[a]

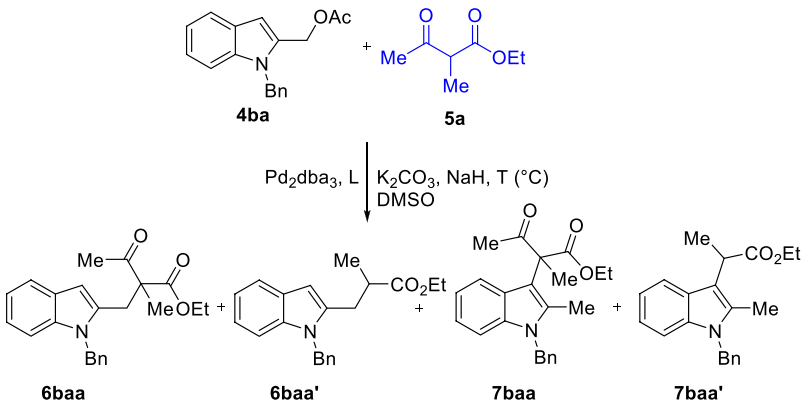

Entry[b]	Ligand	T (°C)	t (h)	6baa (%)	6baa′ (%)	7baa (%)	7baa′ (%)	Overall yield (%)	C1′/C3
1	dppp	120	24	31	51	2		84	97/3
2	dppp	100	24	44	49	3		96	97/3
3	dppf	100	2	53	42	3		98	97/3
4	DavePhos	120	24	2	53	3		57	96/4
5[c]	SPhos	100	3	47	36	5		88	96/4

[a]Unless otherwise stated, reactions were carried out on a 0.30 mmol scale under an argon atmosphere using 0.02 equiv of Pd_2dba_3, 0.08 equiv of monodentate ligand or 0.04 of bidentate ligand, 1.5 equiv of **5a**, 1.5 equiv of K_2CO_3, and 1.7 equiv of NaH in 2.5 mL of anhydrous DMSO. [b]Yields are given for isolated products. [c]**4ba** was recovered in 12% yield.

RESULTS AND DISCUSSION

To prevent the formation of 1,2-dihydro-3*H*-pyrrolo[1,2-*a*]indol-3-ones **3** previously reported by us (Scheme 3b),[10] we started our investigation by exploring the palladium-catalyzed reaction of *N*-protected (1*H*-indol-2-yl)methyl acetate **4** with ethyl 2-methyl-3-oxobutenoate **5a**. Surprisingly, with (1-tosyl-1*H*-indol-2-yl)methyl acetate **4aa** we observed that, besides the formation of the expected coupling reaction at the C1′ position, an unprecedented attack at the C3 position of the plausible η^3-indolyl-palladium intermediate can occur (Scheme 5).

With the aim to achieve product selectivity control, we tested the reaction using a variety of ligands, bases, and solvents (Table 1). Ligands showed significant influence on the reactivity and selectivity. The bidentate bisphosphine ligand dppf was effective in allowing the conversion of the starting **4aa** up to 98% with the formation of the substitution products in C1′/C3 ratio 46/54 when the reaction was carried out in DMSO at 100 °C in the presence of a mixture of K_2CO_3/NaH (Table 1, entry 8). Poorer conversion was observed when Cs_2CO_3 or K_2CO_3 was used as a base under the same reaction conditions (Table 1, entries 2 and 3) while Li_2CO_3 was found to be ineffective (Table 1, entry 1). Comparable results were observed when DMF was used instead of DMSO (Table 1, entries 6 and 7), but THF was unsuitable, although it achieved a better C1′ selectivity (Table 1, entries 4 and 5). The use also of only NaH in DMF gave poorer conversion compared to the use of the mixture of K_2CO_3/NaH under the same conditions (Table 1, entry 6 vs entry 7). Up to quantitative conversion of the starting **4aa** was observed when the reaction with ethyl 2-methyl-3-oxobutenoate **5a** (1.5 equiv) was carried out in DMSO at 100 °C in the presence of K_2CO_3 (1.5 equiv), NaH (1.7 equiv), $Pd_2(dba)_3$ (0.08 equiv), and the bidentate ligand dppp (0.04 equiv) (Table 1, entry 11). While dpmm was ineffective (Table 1, entry 9), the comparison with the results observed with the use of dppe instead of dppp (Table 1, entries 10 and 11) highlighted the importance of a wide bite angle of the ligand on the reactivity and regioselectivity. Indeed, the use of bulkier Xantphos achieved, besides the quantitative conversion of **4aa**, the reversion of the regioselectivity toward the prevalent formation of the C3-substituted products (Table 1, entry 12). Similar switching of the regioselectivity toward the C3-substituted products resulted when the reaction occurred in the presence of monophosphine ligands bearing a dialkyl biaryl framework (Table 1, entries 13−18) in contrast with those obtained in the presence of MePhos and JohnPhos (Table 1, entries 19 and 20). The employment of $[Pd(\eta^3\text{-}C_3H_3)Cl]_2$ with DavePhos instead of Pd_2dba_3 was also attempted (Table 1, entries 15 and 16). However, both steric and electronic properties of the ligands determined the reactivity and the regioselective outcome (Table 1, entries 21−25).[12] The formation of the products **6aaa′** and **7aaa′** should derive from a retro Claisen reaction under the reaction conditions.[13]

Subsequently, we used *N*-benzyl derivative **4ba** to explore the effect of a different *N*-protective group on the control of the regioselective outcome. In all cases examined, we observed high regioselective formation of products functionalized at the C1′ position in high overall yield (Table 2).

When the optimized reaction conditions [Pd_2dba_3, SPhos or dppf, K_2CO_3, and NaH in anhydrous DMSO] were extended to a variety of functionalized (*N*-substituted-1*H*-indol-2-yl)methyl acetate **4**, comparative experiments demonstrated the influence of the *N*-benzyl group on directing the regioselective outcome regardless of the feature of the substituent on the aryl ring of the starting acetate (Table 3).

The study of the influence of the feature of the carbon soft pronucleophile on the reaction outcome showed that the reaction of the *N*-benzyl derivative **4ba** with the 2-methylethylmalonate **5b** afforded only the C1′-substituted products in moderate yield under the standardized reaction conditions [Pd_2dba_3, SPhos or dppf, K_2CO_3, and NaH in anhydrous DMSO] while the regioselectivity control failed to occur with the more reactive *N*-tosyl derivative **4aa** (Table 4).

By contrast, both compounds **6bac** (Table 5, entry 2) and **6aac** (Table 5, entry 6) were isolated in satisfactory yield

https://doi.org/10.1021/acsomega.4c02409
ACS Omega XXXX, XXX, XXX−XXX

Table 3. Reaction of Functionalized Derivatives 4 with Ethyl 2-Methyl-3-oxobutenoate 5a[a]

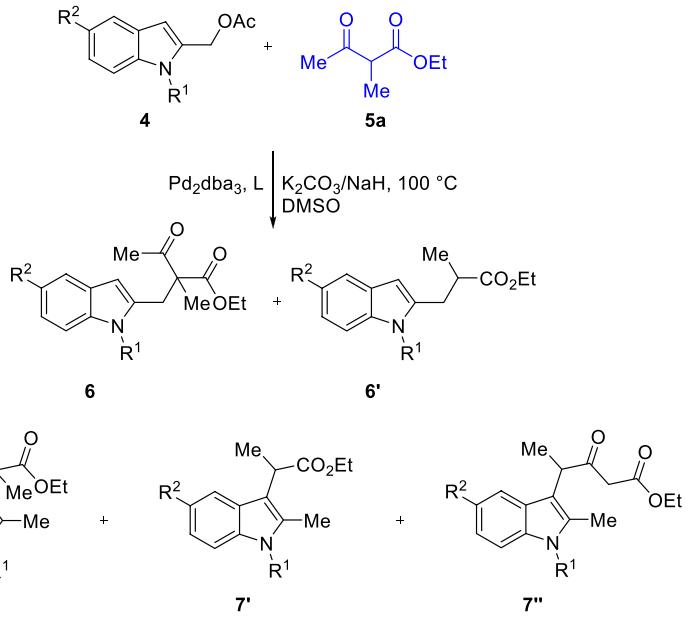

Entry[b]	R[1]	R[2]	4	Ligand	t (h)	6 (%)	6′ (%)	7 (%)	7′ (%)	7″ (%)	Overall yield (%)	C1′/C3
1	Bn	Cl	**4bb**	dppf	1	**6bba** (79)	**6bba′** (9)	**7bba** (/)	**7bba′** (/)	**7bba″** (/)	88	100/0
2	Ts	OMe	**4ab**	dppf	2	**6aba** (44)	**6aba′** (4)	**7aba** (26)	**7aba′** (3)	**7aba″** (8)	85	57/43
3[c]	Ts	OMe	**4ab**	SPhos	24	**6aba** (10)	**6aba′** (9)	**7aba** (18)	**7aba′** (13)	**7aba″** (3)	53	38/62
4	Bn	OMe	**4bc**	dppf	2	**6bca** (46)	**6bca′** (15)	**7bca** (/)	**7bca′** (/)	**7bca″** (/)	71	100/0
5	Ts	Me	**4ac**	dppf	20	**6aca** (36)	**6aca′** (17)	**7aca** (36)	**7aca′** (4)	**7aca″** (8)	100	53/47
6	Ts	Me	**4ac**	Sphos	20	**6aca** (14)	**6aca′** (10)	**7aca** (46)	**7aca′** (20)	**7aca″** (7)	98	25/75
7[d]	Bn	Me	**4bd**	dppf	1	**6bda** (40)	**6bda′** (21)	**7bda** (/)	**7bda′** (/)	**7bda″** (/)	61	100/0
8	Ts	Ph	**4ad**	dppf	6	**6ada** (24)	**6ada′** (3)	**7ada** (38)	**7ada′** (4)	**7ada″** (7)	76	35/65
9	Bn	Ph	**4be**	dppf	3	**6bea** (86)	**6bea′** (13)	**7bea** (/)	**7bea′** (/)	**7bea″** (/)	99	100/0

[a]Unless otherwise stated, reactions were carried out on a 0.30 mmol scale under an argon atmosphere using 0.02 equiv of Pd_2dba_3, 0.08 equiv of SPhos or 0.04 of dppf, 1.5 equiv of **5a**, 1.5 equiv of K_2CO_3, and 1.7 equiv of NaH in 2.5 mL of anhydrous DMSO. [b]Yields are given for isolated products. [c]**4ab** was recovered in 5% yield. [d](1-Benzyl-1*H*-indol-2-yl)methanol **11ba** was isolated in 5% yield.

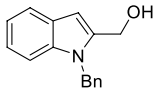

11ba

through the palladium-catalyzed reaction of the indolylmethyl acetates **4aa**−**4ba** with the methyl Meldrum's acid **5c** via sequential attack of the corresponding enolate at the C1′ position/elimination of acetone and CO_2 (Table 5).[14]

Interestingly, the heptanoic acid derivatives **13a**,**b** were effectively obtained under optimized reaction conditions (Table 6, entries 2 and 4) through the sequential C1′ regioselective substitution/retro-Dieckmann reactions of acetates **4** with 2-methylcyclohexane-1,3-dione **5d**.[15] Only traces of 2-methyl-2-((1-tosyl-1*H*-indol-2-yl)methyl)cyclohaxane-1,3-dione **6aad** were detected (Table 6, entry 5).

The potential of the strategy aimed at the diversity-oriented synthesis of indole derivatives is further highlighted by the investigation of the palladium-catalyzed regioselective functionalization of (1-substituted-1*H*-indol-3-yl)methyl acetates **8a** with a variety of carbon pronucleophiles. Indeed, ethyl 2-methyl-3-oxo-2-((1-tosyl-1*H*-indol-3-yl)methyl)butanoate **9aa** was isolated in 98% yield by reacting acetate **8a** in MeCN in the presence of Pd_2dba_3/dppf as the catalytic system (Table 7, entry 5) or by carrying out the reaction using [Pd(η^3-C_3H_5)Cl]/XPhos and 3 equiv of **5a** at 120 °C in a mixture 4:1 of MeCN/THF solvents (Table 7, entry 4). The formation of the product by a base-promoted reaction can be ruled out by recovering the starting acetate under metal-free conditions (Table 7, entry 1). The choice of the suitable reaction medium also achieved the suppression of the retro Claisen reaction, leading to the conversion of **9aa** to ethyl 2-methyl-3-(1-tosyl-1*H*-indol-3-yl)propanoate **9aa′** which prevailed as the main product in a 4:1 DMSO/THF mixture of solvent (Table 7, entry 3).

Furthermore, after a brief screening with **8a** and ethyl 2-methylmalonate **5b**, we found that the best conditions were the same as used with **5a** [Pd_2dba_3, XPhos, and K_2CO_3 in MeCN/THF] (Table 8, entry 6). After prolonged reaction times, the hydrolysis of the tosyl group can also be observed to some extent (Table 8, entries 3−5).

Then, the substituted *N*-Ts-indol-3-ylmethyl acetates **8** reacted under the standardized reaction conditions with the β-ketoesters and malonates **5a**−**g** to afford the corresponding products **9** in moderate to high yield (Table 9).

A brief exploration of the palladium-catalyzed reaction of *N*-Ts-indol-3-ylmethyl acetates showed that the reaction of **8** with diketones **5d** and **5h** gave the corresponding 2-methyl-2-(1-

https://doi.org/10.1021/acsomega.4c02409
ACS Omega XXXX, XXX, XXX−XXX

Table 4. Reaction of Functionalized Derivatives 4 with 2-Methylethyl Malonate 5b[a]

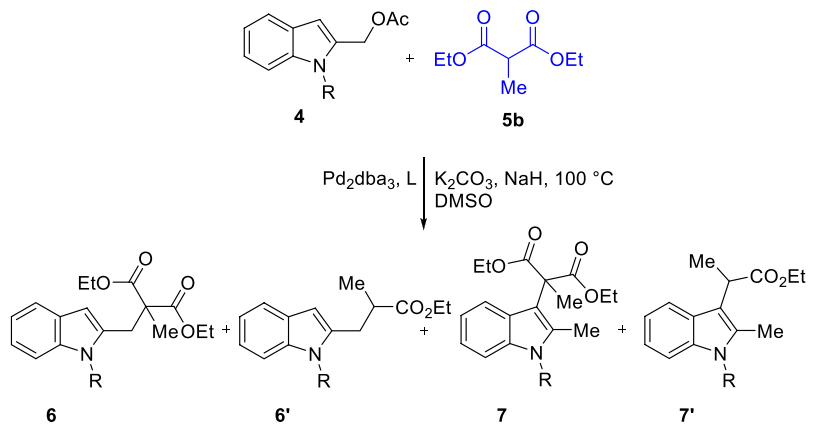

Entry[b]	R	4	Ligand	*t* (h)	6 (%)	6′ (%)	7 (%)	7′ (%)	Overall yield (%)	C1′/C3
1[c,d]	Bn	**4ba**	dppf	24	**6bab** (39)	**6baa′** (7)	**7bab** (/)	**7baa′** (/)	46	100/0
2[e]	Bn	**4ba**	SPhos	24	**6bab** (27)	**6baa′** (26)	**7bab** (/)	**7baa′** (/)	53	100/0
3[f,g,h]	Ts	**4aa**	dppf	24	**6aab** (29)	**6aaa′** (3)	**7aab** (35)	**7aaa′** (/)	84	58/42
4[h,i,j]	Ts	**4ba**	SPhos	5	**6aab** (18)	**6aaa′** (/)	**7aab** (43)	**7aaa′** (/)	88	51/49

[a]Unless otherwise stated, reactions were carried out on a 0.30 mmol scale under an argon atmosphere using 0.02 equiv of Pd_2dba_3, 0.08 equiv of ligand, 1.5 equiv of **5b**, 1.5 equiv of K_2CO_3, and 1.7 equiv of NaH in 2.5 mL of anhydrous DMSO. [b]Yields are given for isolated products. [c](1-Benzyl-1*H*-indol-2-yl)methanol **11ba** was isolated in 17% yield. [d]**4ba** was recovered in 12% yield. [e](1-benzyl-1*H*-indol-2-yl)methanol **11ba** was isolated in 11% yield. [f]**3** was isolated in 12% yield. [g]**12** was isolated in 5% yield. [h]Overall yield and C1′/C3 ratio were calculated including **3** and **12**. [i]**3** was isolated in 16% yield. [j]**12** was isolated in 11% yield.

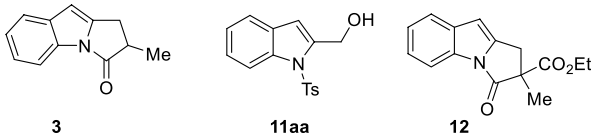

Table 5. Reaction of Functionalized Derivatives 4 with Methyl Meldrum's Acid 5c[a]

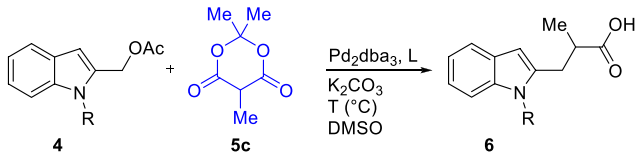

Entry[b]	R	4	Ligand	*T* °(C)	*t* (h)	6 (%)
1[c]	Bn	**4ba**	dppf	100	24	**6bac** (/)
2[d]	Bn	**4ba**	dppf	120	9	**6bac** (60)
3[e,f]	Ts	**4aa**		100	24	**6aac** (/)
4[e,g,h]	Ts	**4aa**		120	24	**6aac** (/)
5[i,j]	Ts	**4aa**	dppf	100	72	**6aac** (/)
6	Ts	**4aa**	dppf	120	2	**6aac** (62)
7[k]	Ts	**4aa**	dppf	120	24	**6aac** (20)
8	Ts	**4aa**	XantPhos	120	24	**6aac** (31)
9[l,m]	Ts	**4aa**	SPhos	120	42	**6aac** (18)

[a]Unless otherwise stated, reactions were carried out on a 0.30 mmol scale under an argon atmosphere using 0.02 equiv of Pd_2dba_3, 0.08 equiv of ligand, 1.5 equiv of **5c**, and 1.5 equiv of K_2CO_3 in 2.5 mL of anhydrous DMSO. [b]Yields are given for isolated products. [c]**4ba** was recovered in 77% yield. [d]**4ba** was recovered in 5% yield. [e]The reaction was carried out without Pd_2dba_3. [f]**4aa** was recovered in 80% yield. [g]**4aa** was recovered in 37% yield. [h]1-Tosyl-1*H*-indol-2-yl)methanol **11aa** was isolated in 6% yield. [i]**4aa** was recovered in 77% yield. [j]**3** was isolated in 8% yield. [k]Reaction was carried out in the presence of Cs_2CO_3. [l]**4aa** was recovered in 16% yield. [m]**3** was isolated in 18% yield.

Table 6. Reaction of Functionalized Derivatives 4 with 2-Methylcyclohexane-1,3-dione 5d[a]

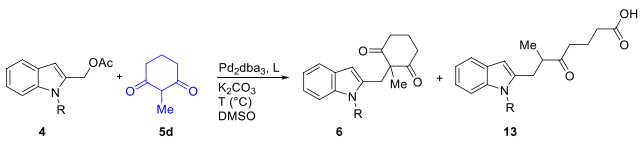

Entry[b]	R	4	Ligand	*T* °(C)	*t* (h)	13 (%)
1[c]	Bn	**4ba**	dppf	120	3	**13b** (68)
2[d]	Ts	**4aa**	dppf	120	72	**13a** (27)
3[e]	Ts	**4aa**	dppf	100	72	**13a** (20)
4[c]	Ts	**4aa**	dppf	100	24	**13a** (64)
5[c,f]	Ts	**4aa**	dppf	120	2	**13a** (19)
6[c,g]	Ts	**4aa**	SPhos	100	18	**13a** (/)

[a]Unless otherwise stated, reactions were carried out on a 0.30 mmol scale under an argon atmosphere using 0.02 equiv of Pd_2dba_3, 0.08 equiv of SPhos or 0.04 equiv of dppf, 1.5 equiv of **5d**, and 1.5 equiv of K_2CO_3 in 2.5 mL of anhydrous DMSO. [b]Yields are given for isolated products. [c]The reaction was carried out with potassium salt of **5d**. [d]**4aa** was recovered in 40% yield. [e]**4aa** was recovered in 40% yield. [f]**6aad** was detected in traces. [g]**4aa** was recovered in 54% yield.

tosyl-1*H*-indol-3-yl)methyl)cyclohexane-1,3-dione **9ad** and 3-methyl-3-(1-tosyl-1*H*-indol-3-yl)methyl)pentane-2,4-dione **9ah** in 91% and 80% yields, respectively (Table 10, entries 1 and 2). The presence of chlorine on the benzene ring as substituent is well tolerated, while the methoxy group determined an increase in the amount of the retro Claisen derivative **9′** (Table 10, entries 3 and 4).

https://doi.org/10.1021/acsomega.4c02409
ACS Omega XXXX, XXX, XXX−XXX

Table 7. Optimization Studies for the Reaction of 11a with Ethyl 2-Methylacetoacetae 5a[a]

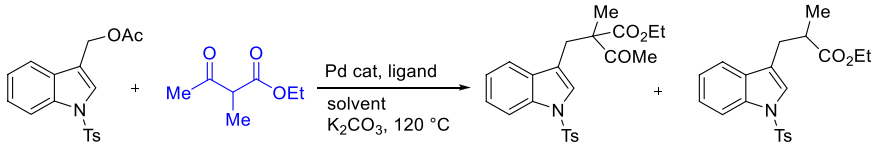

8a 5a 9aa 9aa'

Entry[b]	Pd cat.	Ligand	Solvent	*t* (h)	9aa (%)	9aa′ (%)
1[c]			DMSO	5	9	
2	$Pd_2(dba)_3$	dppf	DMSO	2	75	9
3	$Pd_2(dba)_3$	SPhos	DMSO/THF 4:1	24	20	49
4	$[Pd(C_3H_5)Cl]_2$	XPhos	MeCN/THF 4:1	24	98	
5	$Pd_2(dba)_3$	dppf	MeCN	8	98	

[a]Unless otherwise stated, reactions were carried out on a 0.29 mmol scale under an argon atmosphere using 0.04 equiv of Pd, 0.04 equiv of ligand, 3 equiv of **5a**, and 2 equiv of K_2CO_3 in 2.5 mL of anhydrous solvent at 120 °C. [b]Yields are given for isolated products. [c]**8a** was recovered in 53%

Table 8. Optimization Studies for the Reaction of 8a with Ethyl 2-Methylmalonate 5b[a]

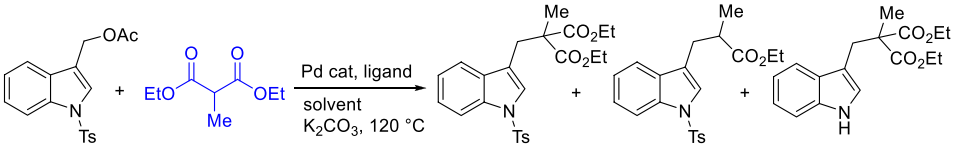

8a 5b 9ab 9aa' 9ab''

Entry[b]	Pd cat	Ligand	Solvent	*t* (h)	9ab (%)	9aa′ (%)	9ab″ (%)
1	$Pd_2(dba)_3$	dppf	DMSO	4	55	6	
2[c]	$Pd_2(dba)_3$	dppf	MeCN	2	84	9	
3[d]	$Pd_2(dba)_3$	dppf	1,4-dioxane	29	41	49	4
4	$[Pd(C_3H_5)Cl]_2$	SPhos	DMSO/THF 4:1	29	45	14	11
5[e]	$[Pd(C_3H_5)Cl]_2$	SPhos	MeCN/THF 4:1	8	69		11
6	$[Pd(C_3H_5)Cl]_2$	XPhos	MeCN/THF 4:1	2.5	81		

[a]Unless otherwise stated, reactions were carried out on a 0.29 mmol scale under an argon atmosphere using 0.04 equiv of Pd, 0.04 equiv of ligand, 2 equiv of **5b**, and 2 equiv of K_2CO_3 in 2.5 mL of anhydrous solvent. [b]Yields are given for isolated products. [c]**14** was isolated in 7%. [d]**14** was isolated in 15% yield. [e]**14** was isolated in 8% yield.

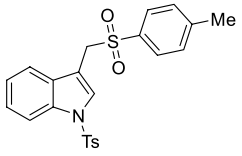

14

Finally, the study of the palladium-catalyzed reaction of *N*-Ts-indol-3-ylmethyl acetates with Meldrum's acid derivatives **5c** demonstrated the general effectiveness of the regioselective diversity orientated synthesis of indoles of the procedure (Table 11).

Intrigued by the experimental results of the *N*-free and *N*-protected indolylmethyl acetates with soft carbon pronucleophiles, we performed quantum-chemical calculations as reported in the Computational Details, aimed to provide insight into the reaction pathways enabling us to achieve the product selectivity control and to clarify the differences between the palladium-catalyzed vs the metal-free processes previously reported by us (Schemes 2 and 3).[6−10]

All the calculations were performed in the framework of the Density Functional Theory using the wB97XD functional, corresponding to a range-separated version of Becke's 97 functional with additional dispersion correction,[16] with different basis sets: geometry optimizations were carried out with the 6-31G* for the atoms of the first, second, and third row elements, the Los Alamos Effective Core Potential with a double-z basis set (LANL2DZ) was used for palladium.[17] Energies were then refined through single point calculations, adding a diffusion function (6-31+G*) to the second and third row elements. All the structures were optimized in the gas phase and characterized, through the calculation of the mass-weighted Hessian matrix, as minima (all positive eigenvalues of the Hessian matrix) or transition structures (1 negative eigenvalue of the Hessian matrix). The Gibbs molar free energy ($G_{X,gas}$) was then calculated, using the previous geometries and harmonic frequencies, for each species in the gas phase at 100 °C and at the concentration of 1.0 mol/L (standard state) using the standard statistical-mechanical relations. Finally the solvation in DMSO, i.e., excess molar free energy ($G_{X,solv}$), was calculated within the mean-field approximation in DCE using the Polarizable Continuum Model (PCM).[18] Within this approximation, the molar free energy (G_X) for the generic X species in

https://doi.org/10.1021/acsomega.4c02409
ACS Omega XXXX, XXX, XXX−XXX

Table 9. Reaction of *N*-Ts-indol-3-ylmethyl Acetates 8 with *β*-Ketoester and Malonates 5[a]

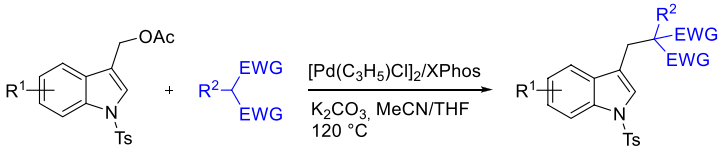

8 **5** **9**

Entry[b]	Catalytic system	R^1	8	5	t (h)	9 (%)
					5.5	**9be** (80)
1	A	5-NO_2	**8b**	 **5e**		
2[c]	A	5-NO_2	**8b**	 **5f**	1	**9bf** (87)
3	A	5-OMe	**8c**	 **5e**	15	**9ce** (82)
	B				32	**9ce** (89)
4	A	5-OMe	**8c**	 **5f**	1.5	**9cf** (93)
5	A	5-OMe	**8c**	 **5a**	24	**9ca** (99)
6[d]	A	6-Cl	**8d**	 **5e**	9	**9de** (27)
	B				25	**9de** (77)
7[e]	A	6-Cl	**8d**	 **5f**	24	**9df** (30)
	B				6	**9df** (80)
8	B	6-Cl	**8d**	 **5a**	24	**9da** (90)
9	A	5-NO_2	**8b**	 **5b**	24	**9bb** (79)
10	A	5-OMe	**8c**	 **5b**	7	**9cb** (78)
11[f]	A	6-Cl	**8d**	 **5b**	56	**9db** (55)
12	B				24	**9db** (77)
13[g]	A	H	**8a**	 **5g**	4	**9ag** (59)
14	A	H	**8a**	 **5e**	5	**9ae** (87)
15	A	H	**8a**	 **5f**	0.5	**9af** (91)

[a]Unless otherwise stated, reactions were carried out on a 0.29 mmol scale under an argon atmosphere at 100 °C using 2.0 equiv of **5**, 0.025 equiv of $[Pd(C_3H_5Cl)]_2$, 0.05 equiv of XPhos, and 2 equiv of K_2CO_3 in 2.5 mL of MeCN/THF mixture (4:1) [Condition A] or 0.025 equiv of $[Pd(C_3H_5Cl)]_2$ and 0.025 equiv of dppf in MeCN [Condition B]. [b]Yields are given for isolated products. [c]**8c** was recovered in 10% yield. [d]**8c** was recovered in 56% yield. [e]**8d** was recovered in 24% yield. [f]**8d** was recovered in 9% yield. [g]**15** was isolated in 12% yield.

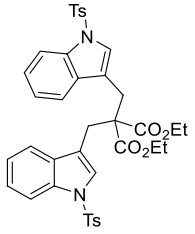

15

solution was simply evaluated through the usual equation $G_X = G_{X,gas} + G_{X,solv} + RT \ln [X]$. Of course, in the standard state reported in all the figures, [X] = 1.0 M for all the species in solution. All the quantum-chemical calculations were carried out with the Gaussian09 package.[19] All the Cartesian coordinates of the optimized geometries are collected in the Supporting Information.[19] First of all we have modeled the initial stage of the C1′ vs C3 nucleophilic attack on the indolyl-palladium intermediate (see Scheme 5). For this purpose, we have utilized 2-methylmalonaldehyde **5l** as nucleophile, two PH_3 groups as simplified palladium ligands, and three different *N*-substituents (R = H, Ts, and Bn). The results are reported in Figures 1 (R = H), 2 and 3 (R = Ts), and 4 (R = Bn). In all the cases, we have observed that the channel leading to the C1′-substituted

https://doi.org/10.1021/acsomega.4c02409
ACS Omega XXXX, XXX, XXX−XXX

Table 10. Reaction of *N*-Ts-indol-3-ylmethyl Acetates 8 with 1,3-Diketones 5d,h[a]

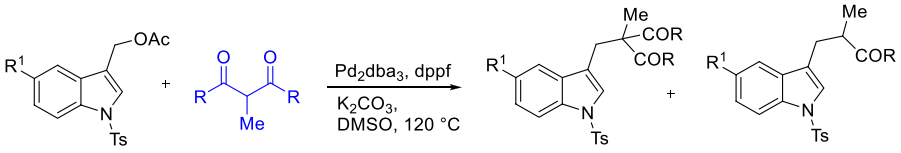

8 5 9 9'

Entry[b]	R^1	8	5	t (h)	9 (%)	9'(%)
1	H	8a		1.5	9ad (91)	/
2	H	8a		1	9ah (80)	3
3	5-OMe	8c		2.5	9ch (43)	37
4	6-Cl	8d		24	9dh (71)	18

[a]Unless otherwise stated, reactions were carried out on a 0.29 mmol scale under an argon atmosphere using 0.04 equiv of Pd, 0.04 equiv of ligand, 3 equiv of **5**, and 2 equiv of K_2CO_3 in 2.5 mL of anhydrous solvent. [b]Yields are given for isolated products.

Table 11. Reaction of *N*-Ts-indol-3-ylmethyl Acetates 8 with Meldrum's Acid Derivatives 5[a]

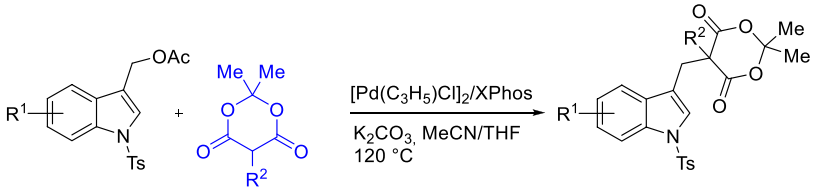

8 5 9

Entry[b]	R^1	8	R^2	*t* (h)	9 (%)
1	H	8a	Me	8	9ac (98)
2	H	8a	$CH_2(4\text{-}OMeC_6H_4)$	0.5	9ai (98)
3	H	8a	$CH_2(4\text{-}SMeC_6H_4)$	7	9aj (80)
4	H	8a	CH_2(2-furyl)	1	9ak (99)
5	5-NO_2	8b	Me	1.5	9bc (88)
6	5-OMe	8c	Me	0.5	9cc (95)
7	5-OMe	8c	$CH_2(4\text{-}OMeC_6H_4)$	0.5	9ci (95)
8	5-OMe	8c	$CH_2(4\text{-}SMeC_6H_4)$	6	9cj (83)
9	5-OMe	8c	CH_2(2-furyl)	1.5	9ck (91)
10	6-Cl	8d	$CH_2(4\text{-}OMeC_6H_4)$	25	9di (70)
11	6-Cl	8d	$CH_2(4\text{-}SMeC_6H_4)$	6.5	9dj (75)
12	6-Cl	8d	CH_2(2-furyl)	24	9dk (89)

[a]Unless otherwise stated, reactions were carried out on a 0.29 mmol scale under an argon atmosphere at 120 °C using 1.5 equiv of **5**, 0.025 equiv of $[Pd(C_3H_5Cl)]_2$ and 0.05 equiv of XPhos, and 2 equiv of K_2CO_3 in 2.5 mL of MeCN/THF mixture (4:1). [b]Yields are given for isolated products.

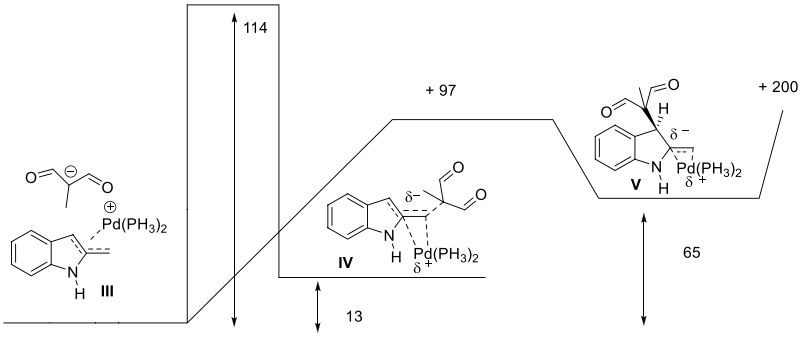

Figure 1. Standard free energy diagram (at 100 °C in DMSO) in kJ/mol.

https://doi.org/10.1021/acsomega.4c02409
ACS Omega XXXX, XXX, XXX−XXX

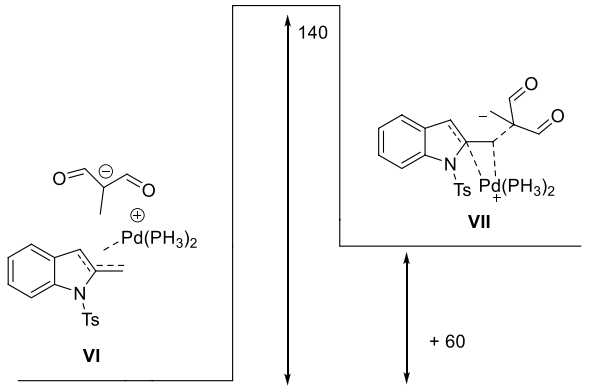

Figure 2. Standard free energy diagram (at 100 °C in DMSO) in kJ/mol.

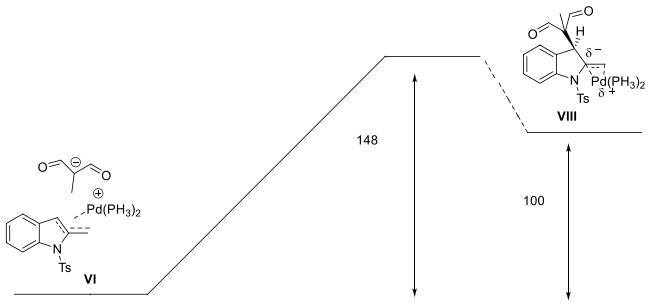

Figure 3. Standard free energy diagram (at 100 °C in DMSO) in kJ/mol.

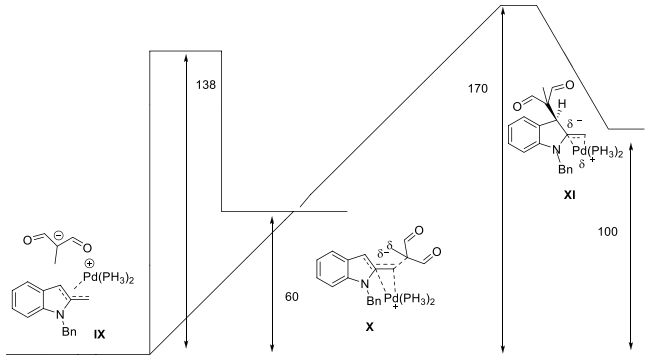

Figure 4. Standard free energy diagram (at 100 °C in DMSO) in kJ/mol.

product is the dominant one. As a matter of fact, irrespective of the height of the initial free energy barrier, the C1′ attack always leads to an intermediate more stable than the intermediate expected upon C3 attack and the barrier for the 1−3 H-shift is always found to be particularly high. In particular, when R = H the formation of the thermodynamically unstable intermediate **V** is a reversible process, which might explain the absence of product substituted at the C3 position. When R = Ts (Figures 2 and 3) we observe that the two intermediates **VII** and **VIII** show rather similar barrier heights; on the other hand, when R = Bn (Figure 4) the formation of intermediate **XI** is characterized by a very high barrier, hence not in disagreement with the experimental data.

Subsequently, we repeated the same calculations for the 3-indolylmethyl-palladium intermediates. Also in this case from the results, depicted in Figures 5 (R = H), 6 (R = Ts), and 7 (R = Bn), we can expect a very high regioselectivity of the nucleophilic attack. As a matter of fact, we observe that (i) a relatively low barrier is found only for the C′$_1$ attack, (ii) the attack at the C2 position does not show any transition structure, (iii) all the reaction intermediates show a similar thermodynamic stability, and (iv) all three reactions are characterized by rather similar barrier heights, slightly higher when R = Ts. All of the results are in agreement with the experimental observations.

We also addressed the question of what could be the actual role of the Pd. In Figure 8 we report the free energy diagram

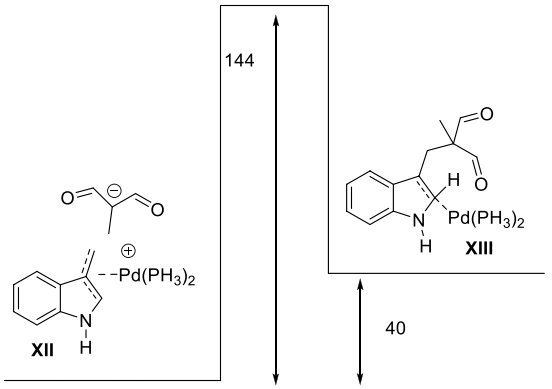

Figure 5. Standard free energy diagram (at 100 °C in DMSO) in kJ/mol.

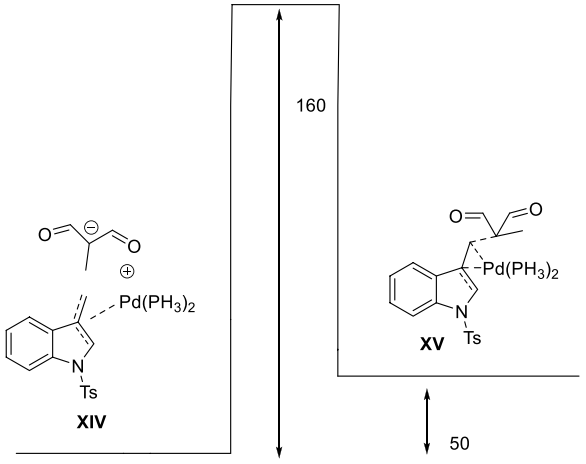

Figure 6. Standard free energy diagram (at 100 °C in DMSO) in kJ/mol.

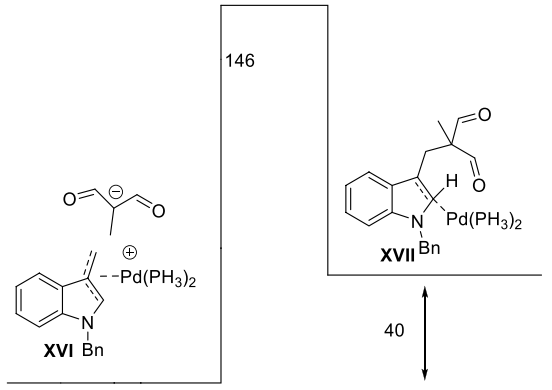

Figure 7. Standard free energy diagram (at 100 °C in DMSO) in kJ/mol.

https://doi.org/10.1021/acsomega.4c02409
ACS Omega XXXX, XXX, XXX−XXX

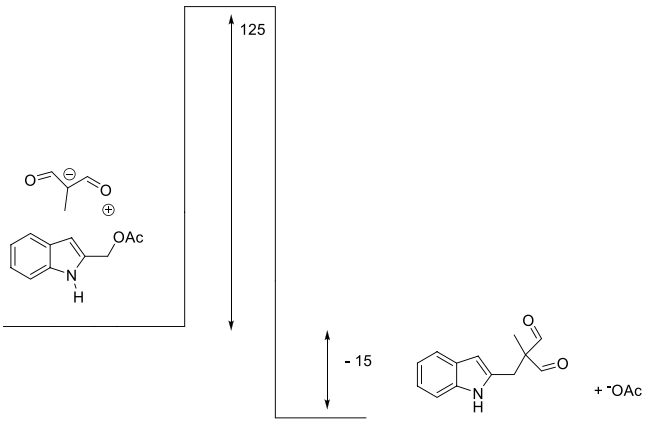

Figure 8. Standard free energy diagram (at 100 °C in DMSO) in kJ/mol.

(maintaining the same temperature and solvent conditions) for the Pd-free reaction with R = H. The result clearly indicates that, at least according to our model, the absence of Pd increases the initial free energy barrier of only 9 kJ/mol, hence suggesting the possible occurrence also of a S_N2 reaction essentially leading to the same product.

Finally, we carried out DFT calculations, in the same temperature and solvent conditions, to provide thermodynamic information concerning additional aspects that could help in rationalizing the possibility of alternative Pd-free reaction pathways involving indolylmethyl cations **XVIII** and**XIX**. As reported in Figure 9, the calculated relative stability, and hence the possible presence at equilibrium, of the indolylmethyl cations indicate that these species under the experimental conditions modeled by our calculations show molar ratios of 4.5×10^{-5} and 3.0×10^{-3}, respectively. The same conclusions could be reached for the possible formation of intermediate **I** by deprotonation with a Bronsted base.

CONCLUSIONS

The palladium-catalyzed reaction of *N*-protected indolylmethyl acetates with different classes of soft carbon pronucleophiles has been investigated. The role of protecting groups, nucleophiles, and ligands in the selective attack on the plausible η^3-indolylpalladium intermediate has been deeply studied. Generally, while with 3-indolylmethyl acetates the nucleophilic substitutions occur exclusively at the exomethyl position, with 2-indolylmethyl acetates the regiochemical outcome could be influenced by the choice of the ligand and protecting group.

Quantum-chemical calculations have been performed to provide insight into the reaction pathways confirming the key role of the palladium catalysis and highlighting the differences between the catalyzed and uncatalyzed processes.

EXPERIMENTAL SECTION

General information, experimental procedures, spectral data of starting materials, final compounds, and spectra copies of synthesized compounds are reported in the Supporting Information.

General Experimental Procedure for the Reaction of *N*-Protected Indolylmethyl Acetates 4 or 11 with Carbonucleophiles 5. In a 50 mL Carousel Tube Reactor (Radely Discovery Technology) containing a magnetic stirring bar, Pd source (0.006 mmol, 0.02 equiv) and ligand (0.012 mmol, 0.04 equiv) were dissolved in anhydrous solvent (1 mL) and stirred at room temperature for 15 min under argon. Then, *N*-protected indolylmethyl acetate **4** or **11** (0.300 mmol, 1.00 equiv), carbonucleophile **5** (0.450 mmol, 1.50 equiv), and K_2CO_3 (0.450 mmol, 1.50 equiv) were added to the mixture and the reaction was stirred at 100 °C. After completion of the

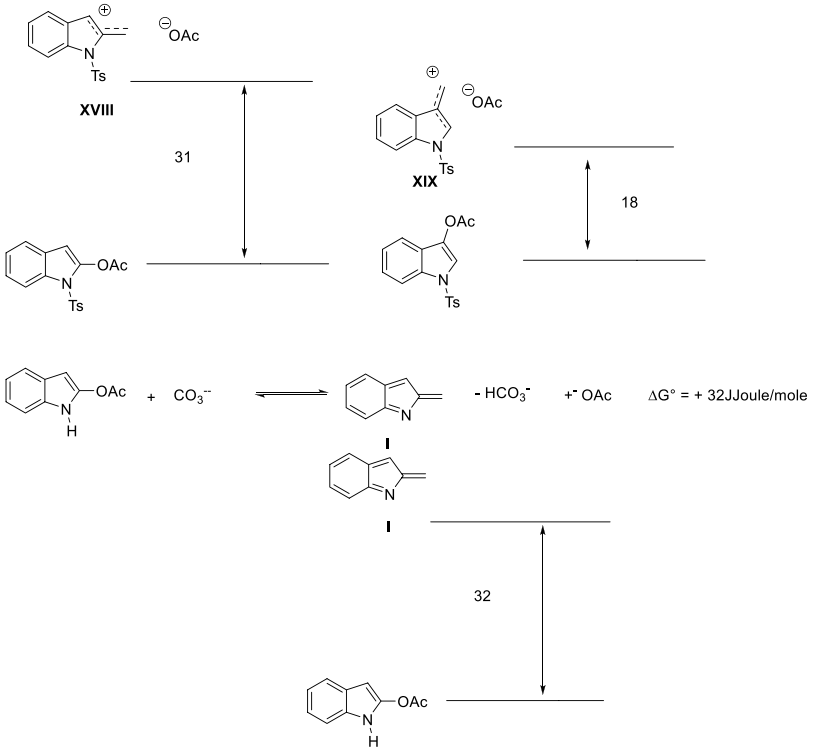

Figure 9. Standard free energy diagram (at 100 °C in DMSO) in kJ/mol.

https://doi.org/10.1021/acsomega.4c02409
ACS Omega XXXX, XXX, XXX−XXX

reaction (monitored by TLC), the mixture was diluted with Et_2O and washed with a $KHSO_4$ solution (10% w/w) and brine (2×). The organic layer was dried over anhydrous Na_2SO_4, filtered, and concentrated under reduced pressure. The crude product was purified by flash chromatography (silica gel, *n*-hexane/AcOEt) to obtain the final products.

With *N*-protected 2-indolylmethyl acetates, depending on the nature of the carbonucleophile, the procedure is slightly modified (generation of carbanion with NaH for *β*-ketoesters, employment of potassium salt with *β*-diketones). For more details, see the Supporting Information.

■ ASSOCIATED CONTENT

Supporting Information

The Supporting Information is available free of charge at https://pubs.acs.org/doi/10.1021/acsomega.4c02409.

General information, reagents and materials, typical procedures for the synthesis of starting materials and final products, characterization data, computational details, atomic coordinates, harmonic frequencies, and copies of ^1H, ^{13}C, and DEPT NMR spectra (PDF)

■ AUTHOR INFORMATION

Corresponding Authors

Giancarlo Fabrizi − *Dipartimento di Chimica e Tecnologie del Farmaco, Sapienza, Università di Roma, 00185 Rome, Italy*; Email: giancarlo.fabrizi@uniroma1.it

Antonia Iazzetti − *Dipartimento di Scienze Biotecnologiche di base, Cliniche Intensivologiche e Perioperatorie, Università Cattolica del Sacro Cuore, 00168 Rome, Italy; Policlinico Universitario 'A. Gemelli' Foundation-IRCCS, Rome 00168, Italy*; orcid.org/0000-0002-7792-774X; Email: antonia.iazzetti@unicatt.it

Authors

Antonio Arcadi − *Dipartimento di Scienze Fisiche e Chimiche, Università degli Studi di L'Aquila, 67100 Coppito, AQ, Italy*; orcid.org/0000-0001-9053-648X

Massimiliano Aschi − *Dipartimento di Scienze Fisiche e Chimiche, Università degli Studi di L'Aquila, 67100 Coppito, AQ, Italy*; orcid.org/0000-0003-2959-0158

Marco Chiarini − *Dipartimento di Bioscienze e Tecnologie Agro-alimentari e Ambientali, Università di Teramo, 64100 Teramo, TE, Italy*; orcid.org/0000-0002-2298-5467

Andrea Fochetti − *Dipartimento di Chimica e Tecnologie del Farmaco, Sapienza, Università di Roma, 00185 Rome, Italy*

Antonella Goggiamani − *Dipartimento di Chimica e Tecnologie del Farmaco, Sapienza, Università di Roma, 00185 Rome, Italy*; orcid.org/0000-0001-8339-4284

Federica Iavarone − *Dipartimento di Scienze Biotecnologiche di base, Cliniche Intensivologiche e Perioperatorie, Università Cattolica del Sacro Cuore, 00168 Rome, Italy; Policlinico Universitario 'A. Gemelli' Foundation-IRCCS, Rome 00168, Italy*; orcid.org/0000-0002-2074-5531

Andrea Serraiocco − *Dipartimento di Chimica e Tecnologie del Farmaco, Sapienza, Università di Roma, 00185 Rome, Italy*

Roberta Zoppoli − *Dipartimento di Chimica e Tecnologie del Farmaco, Sapienza, Università di Roma, 00185 Rome, Italy*

Complete contact information is available at: https://pubs.acs.org/10.1021/acsomega.4c02409

Notes

The authors declare no competing financial interest.

■ ACKNOWLEDGMENTS

We gratefully acknowledge "Sapienza", University of Rome, University of L' Aquila, the Catholic University of Sacred Heart, and PRIN project 2017 "Targeting Hedgehog pathway: virtual screening identification and sustainable synthesis of novel Smo and Gli inhibitors and their pharmacological drug delivery strategies for improved therapeutic effects in tumors" (2017SXBSX4), for financial support. M.A. would like to acknowledge prof. Nico Sanna (University of Tuscia - Viterbo - Italy) for computational facilities and for the use of the package Gaussian16.

■ REFERENCES

(1) Kim, T.; Ha, M. W.; Kim, J. Recent Advances in Divergent Synthetic Strategies for Indole-Based Natural Product Libraries. *Molecules* **2022**, *27* (7), 2171.

(2) Pang, Q.; Zuo, W.-F.; Zhang, Y.; Li, X.; Han, B. Recent Advances on Direct Functionalization of Indoles in Aqueous Media. *Chem. Rec.* **2023**, *23* (3), No. e202200289.

(3) (a) Sachse, F.; Schneider, C. Brønsted Acid Catalyzed (3 + 2)-Cycloaddition of Thioketones and Indole-2-Carbinols Toward Thiazolo[3,4-a]indoles. *Adv. Synth. Catal.* **2022**, *364* (1), 77−81. (b) Zhang, Y.-C.; Jiang, F.; Shi, F. Organocatalytic Asymmetric Synthesis of Indole-Based Chiral Heterocycles: Strategies, Reactions, and Outreach. *Acc. Chem. Res.* **2020**, *53* (2), 425−446. (c) Kataja, A. O.; Masson, G. Imine and iminium precursors as versatile intermediates in enantioselective organocatalysis. *Tetrahedron* **2014**, *70* (46), 8783−8815. (d) Palmieri, A.; Petrini, M.; Shaikh, R. R. Synthesis of 3-substituted indoles via reactive alkylideneindolenine intermediates. *Organic & Biomolecular Chemistry* **2010**, *8* (6), 1259−1270. (e) Li, T.-Z.; et al. Catalytic Asymmetric (3 + 3) Cycloaddition between Different 2-Indolylmethanols. *Sci. China Chem.* **2024**, DOI: 10.1007/s11426-023-1927-3. (f) Shi, Y.-C.; Yan, X.-Y.; Wu, P.; Jiang, S.; Xu, R.; Tan, W.; Shi, F. Design and Application of *m*-Hydroxybenzyl Alcohols in Regioselective (3 + 3) Cycloadditions of 2-Indolylmethanols. *Chin. J. Chem.* **2023**, *41* (1), 27−36. (g) Sheng, F.-T.; Yang, S.; Wu, S.-F.; Zhang, Y.-C.; Shi, F. Catalytic Asymmetric Synthesis of Axially Chiral 3,3′-Bisindoles by Direct Coupling of Indole Rings. *Chin. J. Chem.* **2022**, *40* (18), 2151−2160.

(4) (a) Zhong, X.; Li, Y.; Zhang, J.; Zhang, W.-X.; Wang, S.-X.; Han, F.-S. Formal [3 + 3] cycloaddition of indol-2-yl carbinol with azadiene and the oxidative ring expansion reaction for the synthesis of indole azepinones. *Chem. Commun.* **2014**, *50* (76), 11181−11184. (b) Fu, T.-h.; Bonaparte, A.; Martin, S. F. Synthesis of *β*-heteroaryl propionates via trapping of carbocations with *π*-nucleophiles. *Tetrahedron letters* **2009**, *50* (26), 3253−3257.

(5) (a) Patel, S. M.; P, E. P.; Bakthadoss, M.; Sharada, D. S. Photocatalytic Visible-Light-Induced Nitrogen Insertion via Dual C(sp3)−H and C(sp2)−H Bond Functionalization: Access to Privileged Imidazole-based Scaffolds. *Org. Lett.* **2021**, *23* (2), 257−261. (b) Deng, S.; Qu, C.; Jiao, Y.; Liu, W.; Shi, F. Insights into 2-Indolylmethanol-Involved Cycloadditions: Origins of Regioselectivity and Enantioselectivity. *Journal of Organic Chemistry* **2020**, *85* (18), 11641−11653. (c) Bera, K.; Schneider, C. Brønsted Acid Catalyzed [3 + 2]-Cycloaddition of Cyclic Enamides with in Situ Generated 2-Methide-2*H*-indoles: Enantioselective Synthesis of Indolo[1,2-*a*]-indoles. *Org. Lett.* **2016**, *18* (21), 5660−5663. (d) Bera, K.; Schneider, C. Brønsted Acid Catalyzed [3 + 2]-Cycloaddition of 2-Vinylindoles with In Situ Generated 2-Methide-2H-indoles: Highly Enantioselective Synthesis of Pyrrolo[1,2-a]indoles. *Chem.—Eur. J.* **2016**, *22* (21), 7074−7078. (e) Liu, C.-Y.; Han, F.-S. Organocatalytic asymmetric reaction of indol-2-yl carbinols with enamides: synthesis of chiral 2-indole-substituted 1,1-diarylalkanes. *Chem. Commun.* **2015**, *51* (59), 11844−11847. (f) Gong, Y.-X.; Wu, Q.; Zhang, H.-H.; Zhu, Q.-

https://doi.org/10.1021/acsomega.4c02409
ACS Omega XXXX, XXX, XXX−XXX

N.; Shi, F. Enantioselective construction of a 2,2′-bisindolylmethane scaffold via catalytic asymmetric reactions of 2-indolylmethanols with 3-alkylindoles. *Organic & Biomolecular Chemistry* **2015**, *13* (29), 7993−8000. (g) Qi, S.; Liu, C.-Y.; Ding, J.-Y.; Han, F.-S. Chiral phosphoramide-catalyzed enantioselective synthesis of 2,3′-diindolylarylmethanes from indol-2-yl carbinols and indoles. *Chem. Commun.* **2014**, *50* (62), 8605−8608.

(6) Arcadi, A.; Fabrizi, G.; Fochetti, A.; Ghirga, F.; Goggiamani, A.; Iazzetti, A.; Marrone, F.; Mazzoccanti, G.; Serraiocco, A. Palladium-catalyzed Tsuji−Trost-type reaction of benzofuran-2-ylmethyl acetates with nucleophiles. *RSC Adv.* **2021**, *11* (2), 909−917.

(7) Arcadi, A.; Calcaterra, A.; Chiarini, M.; Fabrizi, G.; Fochetti, A.; Goggiamani, A.; Iazzetti, A.; Marrone, F.; Marsicano, V.; Serraiocco, A. Synthesis of Indole/Benzofuran-Containing Diarylmethanes through Palladium-Catalyzed Reaction of Indolylmethyl or Benzofuranylmethyl Acetates with Boronic Acids. *Synthesis* **2022**, *54* (03), 741−753.

(8) Arcadi, A.; Berden, G.; Ciogli, A.; Corinti, D.; Crestoni, M. E.; De Angelis, M.; Fabrizi, G.; Goggiamani, A.; Iazzetti, A.; Marrone, F.; Marsicano, V.; Oomens, J.; Serraiocco, A. Reactivity of Indolylmethylacetates with N, O, and S Soft Nucleophiles: Evidence of 2-Alkylideneindolenines and 3-Alkylideneindoleninium Generation by ESI-MS and IRMPD Spectroscopy. *Eur. J. Org. Chem.* **2022**, *2022* (43), e202201166.

(9) Goggiamani, A.; Arcadi, A.; Ciogli, A.; De Angelis, M.; Dessalvi, S.; Fabrizi, G.; Iavarone, F.; Iazzetti, A.; Sferrazza, A.; Zoppoli, R. Synthesis of 3-substituted 2,3-dihydropyrazino[1,2-a]indol-4(1*H*)-ones by sequential reactions of 2-indolylmethyl acetates with α-amino acids. *RSC Adv.* **2023**, *13* (15), 10090−10096.

(10) Iazzetti, A.; Arcadi, A.; Dessalvi, S.; Fabrizi, G.; Goggiamani, A.; Marrone, F.; Serraiocco, A.; Sferrazza, A.; Ullah, K. Synthesis of Polysubstituted 1,2-Dihydro-3*H*-pyrrolo[1,2-a]indol-3-ones through Domino Palladium-Catalyzed Reactions of Indol-2-ylmethyl Acetates with 1,3-Dicarbonyl Derivatives. *Catalyst* **2022**, *12* (12), 1516.

(11) (a) Primault, G.; Legros, J.-Y.; Fiaud, J.-C. Palladium-catalyzed benzylic-like nucleophilic substitution of benzofuran-, benzothiophene- and indole-based substrates by dimethyl malonate anion. *J. Organomet. Chem.* **2003**, *687* (2), 353−364. (b) Yang, L.; Chen, X.; Ni, K.; Li, Y.; Wu, J.; Chen, W.; Ji, Y.; Feng, L.; Li, F.; Chen, D. Proton-exchanged montmorillonite-mediated reactions of hetero-benzyl acetates: Application to the synthesis of Zafirlukast. *Tetrahedron letters* **2020**, *61* (29), 152123.

(12) Kamer, P. C. J.; van Leeuwen, P. W. N. M.; Reek, J. N. H. Wide Bite Angle Diphosphines: Xantphos Ligands in Transition Metal Complexes and Catalysis. *Acc. Chem. Res.* **2001**, *34* (11), 895−904.

(13) Yang, D.; Zhou, Y.; Xue, N.; Qu, J. Synthesis of Trifluoromethyl Ketones via Tandem Claisen Condensation and Retro-Claisen C−C Bond-Cleavage Reaction. *Journal of Organic Chemistry* **2013**, *78* (8), 4171−4176.

(14) Arcadi, A.; Calcaterra, A.; Fabrizi, G.; Fochetti, A.; Goggiamani, A.; Iazzetti, A.; Marrone, F.; Mazzoccanti, G.; Serraiocco, A. One-pot synthesis of dihydroquinolones by sequential reactions of *o*-aminobenzyl alcohol derivatives with Meldrum's acids. *Organic & Biomolecular Chemistry* **2022**, *20* (15), 3160−3173.

(15) Duchemin, N.; Cattoen, M.; Gayraud, O.; Anselmi, S.; Siddiq, B.; Buccafusca, R.; Daumas, M.; Ferey, V.; Smietana, M.; Arseniyadis, S. Direct Access to Highly Enantioenriched α-Branched Acrylonitriles through a One-Pot Sequential Asymmetric Michael Addition/Retro-Dieckmann/Retro-Michael Fragmentation Cascade. *Org. Lett.* **2020**, *22* (15), 5995−6000.

(16) Chai, J. D.; Head-Gordon, M. Systematic optimization of long-range corrected hybrid density functionals. *J. Chem. Phys.* **2008**, *128* (8), 084106.

(17) Hay, P. J.; Wadt, W. R. Ab initio effective core potentials for molecular calculations. Potentials for K to Au including the outermost core orbitals. *J. Chem. Phys.* **1985**, *82* (1), 299−310.

(18) Tomasi, J.; Mennucci, B.; Cammi, R. Quantum Mechanical Continuum Solvation Models. *Chem. Rev.* **2005**, *105* (8), 2999−3094.

(19) Frisch, M. J.; Trucks, G. W.; Schlegel, H. B.; Scuseria, G. E.; Robb, M. A.; Cheeseman, J. R.; Scalmani, G.; Barone, V.; Petersson, G. A.; Nakatsuji, H.; Li, X.; Caricato, M.; Marenich, A.; Bloino, J.; Janesko, B. G.; Gomperts, R.; Mennucci, B.; Hratchian, H. P.; Ortiz, J. V.; Izmaylov, A. F.; Sonnenberg, J. L.; Williams-Young, D.; Ding, F.; Lipparini, F.; Egidi, F.; Goings, J.; Peng, B.; Petrone, A.; Henderson, T.; Ranasinghe, D.; Zakrzewski, V. G.; Gao, J.; Rega, N.; Zheng, G.; Liang, W.; Hada, M.; Ehara, M.; Toyota, K.; Fukuda, R.; Hasegawa, J.; Ishida, M.; Nakajima, T.; Honda, Y.; Kitao, O.; Nakai, H.; Vreven, T.; Throssell, K.; Montgomery, J. A., Jr.; Peralta, J. E.; Ogliaro, F.; Bearpark, M.; Heyd, J. J.; Brothers, E.; Kudin, K. N.; Staroverov, V. N.; Keith, T.; Kobayashi, R.; Normand, J.; Raghavachari, K.; Rendell, A.; Burant, J. C.; Iyengar, S. S.; Tomasi, J.; Cossi, M.; Millam, J. M.; Klene, M.; Adamo, C.; Cammi, R.; Ochterski, J. W.; Martin, R. L.; Morokuma, K.; Farkas, O.; Foresman, J. B.; Fox, D. J. *Gaussian 09*, Revision A.02; Gaussian, Inc.: Wallingford, CT, 2016.

https://doi.org/10.1021/acsomega.4c02409
ACS Omega XXXX, XXX, XXX−XXX